Electronic Supplementary Information

Molecular junctions based on intermolecular electrostatic coupling

Zhiwei Yi[a,b], *Stefan Trellenkamp*[a,b], *Andreas Offenhäusser*[a,b], *Dirk Mayer*[a,b*]

[a]Institute of Bio-and Nanosystems (IBN 2), Research Center Jülich, 52425, Germany

[b]JARA-Fundamentals of Future Information Technology, Research Center Jülich, 52425, Germany

AUTHOR EMAIL ADDRESS dirk.mayer@fz-juelich.de

Introduction

The electron transport properties of single molecules are one of the most fascinating subjects in molecular electronics. To measure single molecules, a nanoscale gap with tunable gap size is required to address the molecules individually, forming metal/molecule/metal junctions. For the investigation of biomolecules, hydrogen bond and electrostatically linked molecular systems, nanogaps in aqueous condition are needed to maintain their structural integrity and functionality. Aqueous conditions are also required for the investigation of redox molecules, where an electrochemical gating electrode is used to modulate the electron transport process by controlling their electrochemical potentials.

Although various routines of fabricating nanogaps were proposed,[1] not many methods are available for implementing tunable nanogaps in aqueous conditions.[2-4] Our approach is to integrate an electrochemical cell to the conventional mechanical break junction setup (MBJ), forming an electrochemical mechanical break junction (EC-MBJ). The basic principle of MBJ is to break a gold junction between two electrodes fixed on a substrate, which is usually a microwire fabricated by lithography. By applying a mechanical force on the substrate, the substrate bents and the junction elongates. The thinnest portion of the junction breaks apart, and a nanogap between the two facing electrodes is formed. To add an electrochemical cell to the conventional MBJ is a challenge, since the bending of substrate (several millimetres displacement) would induce many irregular holes and cracks in insulating layer on electrode surface (especially for commonly used stiff dielectric materials like SiOx/SiNx). These cracks would create large and unpredictable parasitic leakage currents at the liquid/electrode interface when the electrolyte penetrates into the insulating layer. This parasitic electrochemical leakage current would interfere with the tunnelling current of the metal/molecule/metal junctions.

Fabrication of electrochemical mechanical break junction with low leakage current

In this work, several approaches were combined to realize highly stable EC-MBJ with low electrochemical leakage current. Firstly, during chip fabrication, a flexible insulating layer (PMMA) was used which adapts better to deformations than rigid SiOx/SiNx layers. Secondly, only a small excess window was opened on the electrode, resulting small area of liquid/electrode interface and low level electrochemical background currents. Thirdly, stable electrodeposited atomic point contacts were established and used as the junction in lieu of the conventional microwires in the mechanical breaking setup. Very little mechanical deformation of the chip was needed to break the atomic point contact to separated electrodes. Thus, the probability of damaging the silicon chip and producing cracks in the insulating layer by mechanical strain was kept minimal. The parasitic electrochemical leakage current caused by the failure of chip structure was also controlled.

A nanoelectrode chip (1×1 cm^2) was mounted on a home-made MBJ setup. An O shape glass ring was glued on the chip by PDMS and filled with appropriate electrolytes, forming a micro electrochemical cell. Tungsten needles were used to touch the contact pads on the chip edge, connecting the nanoelectrodes to the external measuring circuits. A piezo motor (PI GmbH, N-111.3A) was placed under the silicon chip, forming a three-point bending mechanism together with the fixing steel springs .

The nanoelectrode chip was fabricated by electron beam lithography and the surface of the chip was covered by three layers of PMMA (200k/600k/200k) to insulate the gold nanoelectrodes. The chips had a thickness of 230 μm. An access window was opened right over the electrode tips. The initial gap between the facing nanoelectrodes was set to 150 nm. The relatively large gap of this template structure was reduced from 150 nm to atomic point contact by gold electrodeposition. This point connection was subsequently used as nanojunction for the following breaking process in the MBJ setup.

For the electrodeposition, Keithley 4200-SCS semiconductor analyzer (Keithley Instruments Inc.) was used to control the electrochemical potential and monitor the transient current between the

nanoelectrodes. A three-electrode configuration was employed. Two nanoelectrodes were set as source and drain electrode. Ag/AgCl reference electrode (WPI Inc.) was inserted in the electrolyte and set as gate electrode. The deposition solution contained 0.01 mM Chloroauric acid (Aldrich, 99.999%), and 0.5 M Lithium chloride (Aldrich). The deposition was performed until a gold junction was established and the process was controlled by monitoring the source/drain current. A main challenge of this routine lies in the precise control of electrodeposition process. The fabrication of nanogaps by electrodeposition method had been carefully studied and the deposited nanogaps were found stable when the overpotential was set as small as possible during the electrodeposition. Here, electrodeposition was performed at 0.6 V (depositing current starts at 0.7 V) with respect to Ag/AgCl reference electrode,[5] and protruding extensions were generated on the surface with a tip curvature of 10 nm.

If the electrodeposition continued after the atomic contacts were formed, massive junction (over 10 nm in width) would be formed, which could also be used as junction for mechanical breaking. However, the massive junctions were very difficult to break and most of the chips were ruined during breaking process, due to the brittleness of silicon. Using the deposited point contact as junction, the yield was significantly increased and 90% of the chips remained intact after the breaking process. In the following, the electrodeposition and the mechanical breaking process were performed in-situ without interruption (Fig. S1a). The chips were immersed in electrolyte during the whole process to protect the systems from air-born contaminates. Different electrolytes were used in the electrodeposition phase (Chloroauric solution) and in the mechanical breaking process (dilute sulphuric acid). Here, the electrodeposition was stopped when the point contact was formed. An exponential increase of conductance between the source and drain electrode was observed (Fig. S1a, I). After the electrodeposition was stopped, the conductance jumped from 1 G_0 to approximately 4 G_0 then returned to a value between 2 and 3 G_0 (Fig. S1a, II). This conductance jump occurred during the potential change from deposition range to non-deposition range. This fluctuation period lasted about 2 minutes,

then the conductance was settled down and stabilized at this conductance for more than 5 minutes (Fig. S1a, III). During this period, several operations can be performed in-situ. Here, the chip was rinsed by water and the depositing solution was replaced by dilute sulphuric acid. The conductance did not change much when the buffer was replaced (approximately at 400s). This property is in particular of importance for in-situ measurements of molecules in buffer solution of different compositions. The atomic point contact was subsequently broken by the mechanical bending of the chip and exponential decay of conductance was obtained (Fig. S1a, IV). Only slight mechanical bending (10-30 μm, vertically) of silicon chip was required to break the junction.

After the point contacts were formed by deposition, the junctions can be broken and closed mechanically as conventional MBJ setup. Three representative conductance traces recorded during the breaking process were displayed in Fig. S1b. Quantized conductance at 1 G_0 was observed in the conductance traces which indicated the functionality of our setup. The typical exponential decay of conductance demonstrated the pure tunneling response between the two electrodes and reducing factor of 1.7×10^{-5} can be calculated from the tunneling traces. Maximum vertical displacement of 400 μm can be applied on the chip before the chip is destroyed, which allows generating tunable nanogaps from 0 to 4 nm separation, calculated from the reducing factor of this setup. Here, conductance histogram was calculated over 200 breaking curves. A bin size of $5\text{x}10^{-6}$ G_0 was used for the histogram construction. The linear histogram in log-log scale confirmed the pure tunneling response between the bare electrodes (Fig. S1b, inset).

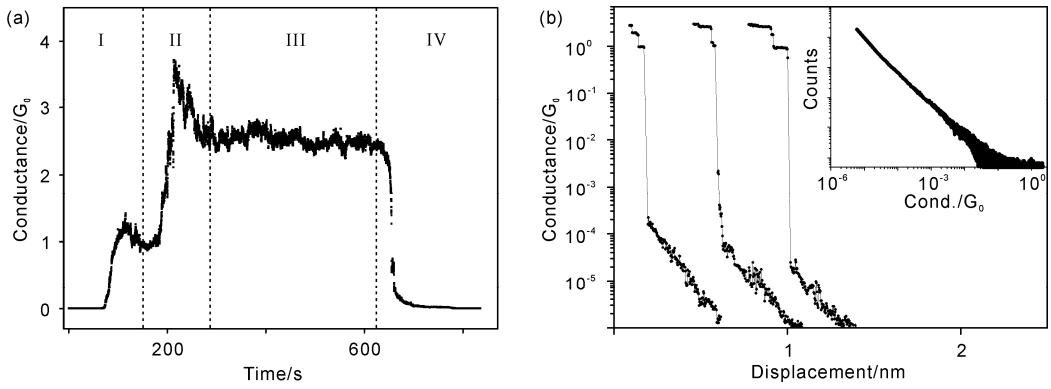

Figure S1. (a) Fabrication of electrochemical break junction setup by combing electrodeposition and mechanical break junction techniques. (I) Electrochemical deposition from a nanogap to point contact. (II) Conductance fluctuation after deposition is stopped. (III) Stable gold point contact over 5 minutes. (IV) Breaking gold contact into nanogaps on mechanical breaking setup. (b) Representative conductance traces recorded during junction breaking process and the corresponding histogram constructed from more than 200 curves.

Electrochemical characterization of the mechanical break junction setup

I-V curves of nanogaps with different gap sizes were studied in dilute sulfuric acid (Fig. S2a). The potential of one electrode was set at 0 V and the potential of the other electrode was swept from 0 V to 0.7 V, with respect to the Ag/AgCl electrode. The accessible potential range is restricted by the electrochemical environment. More positive potential would cause gold oxidation and more negative potential could induce hydrogen evolution reaction. Each curve includes 3 consecutive recordings and no current increase with the number of cycles was observed. The gap sizes were evaluated by Simmons fitting. To further evaluate the electrochemical leakage current of the EC-MBJ, cyclic voltammograms (CVs) were recorded in-situ after the I-V curves were measured (Fig. S2b). The electrodeposited nanojunction was set as working electrode and Au wires immersed in dilute sulphuric acid were used as counter electrode. The reference is Ag/AgCl electrode. The electrochemical current was about 20 pA

measured at potentials where gold is ideal polarizable (below 0.9 V). At higher potentials gold oxidation/reduction occurred. Even under these aggressive conditions, the change of reduction peak current between first CV curve and the second CV curve was within 1%, which indicated that the insulating layer remained nearly intact and the cracks related electrochemical leakage current had no significant influence on the system.

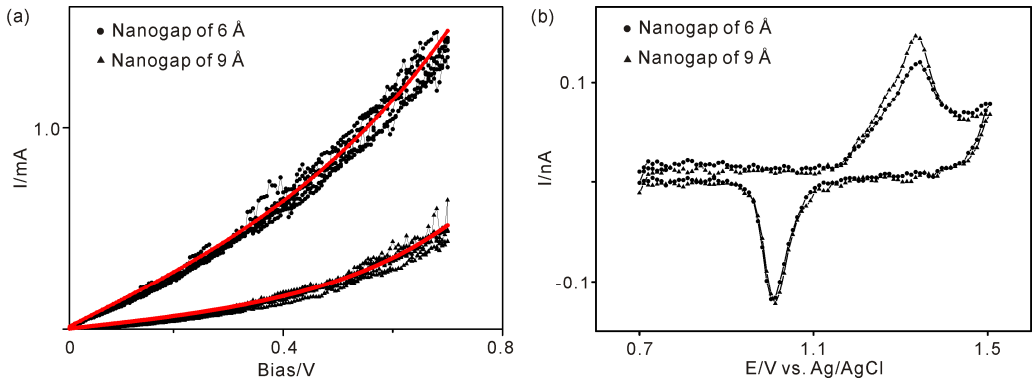

Figure S2. (a) I-V curves of nanogaps at different gap sizes recorded in aqueous solution (black). The gap size was calculated by Simmons fitting (red). (b) Cyclic voltammograms of the electrodes recorded at different gap sizes (100 mV s^{-1}).

Electrochemistry of bare gold electrode at different pHs

Before studying the electrochemistry of cysteamine modified electrode with/without adsorbed FDA at different pHs, the cyclic voltammetry of bare gold electrode in different pHs were performed on a silicon chip (Fig. S3). A gold electrode defined by lithography was used as working electrode (Fig. S3, inset). The leads were buried under insulating PMMA layers and had a contact with the electrolyte when immersing the chip into the electrolyte. Thus, the capacitance current from the leads was inevitably imposed to electrochemical current of the microelectrode when recording the CVs. The redox positions of gold are related to pH value of the electrolyte. From Fig. S4, it becomes obvious that the

gold redox peaks shifted negatively from 0.7 V to 0.2 V when the pH was increased from 2.0 to 10.0 (Fig S4).

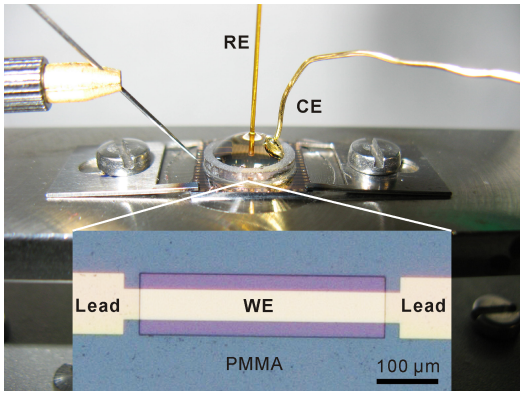

Figure S3. Performing cyclic voltammetry on chip. Working electrode (WE): gold electrode defined on silicon chip encapsulated by PMMA with exposed area of 0.02 mm^2. Counter electrode (CE): gold wire with melting tip. Reference electrode (RE): Ag/AgCl microelectrode. The leads are used to provide electrical connections to the working electrode. Note that only part of the leads is shown in the inset.

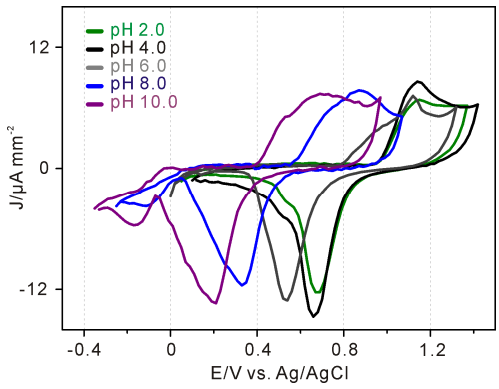

Figure S4. CVs of bare gold electrodes recorded in Britton-Robinson buffer at pH values from 2.0 to 10.0 to evaluate the pH induced potential shift.

Calculation of histograms from conductance traces

Each histogram in Fig. 3b was constructed from 200 conductance curves. The conductance trace is actually a data sheet with two columns of data, the first column is the conductance and the second is the displacements between the two electrodes. The conductance data from 200 conductance traces were extracted and combined to one data set and the histogram of the combined dataset was determined. A bin size of $5x10^{-6}$ G_0 was used to calculate the histograms. The histogram analysis generated a data set with two columns: probability and the conductance values. This histogram was represented in log scale to obtain an overview of the conductance distribution over a large conduction range of five orders of magnitude. Moreover, in log scale, the conductance histogram of pure tunnelling appears as a straight line. This makes it is easier to distinguish the histograms with peaks from histograms of pure tunnelling.

To calculate the position of the peaks observed in the conductance histogram, the histogram with peaks was firstly subtracted by the pure tunnelling histogram to eliminate the background effect; then, the peaks of the subtracted histogram was positioned by Gaussian fitting, according to the work of Schönenberger. The configurations of the molecular junctions are similar: same electrodes, same adsorbed molecules and same type of buffer, except that the pH of buffer is different. Therefore, it is reasonable to assume the decay parameters in the tunnelling equations do not vary a lot and the tunnelling current can be subtracted. This assumption was also confirmed by the same slope of the histograms lines shown in Fig. 3b, since the slope of the histogram in log scale is proportional to the tunnelling decay parameters.

Reference List

1. Li, T.; Hu, W. P.; Zhu, D. B. Nanogap Electrodes. *Adv. Mater.* **2010,** *22*, 286-300.
2. Gruter, L.; Gonzalez, M. T.; Huber, R.; Calame, M.; Schonenberger, C. Electrical conductance of atomic contacts in liquid environments. *Small* **2005,** *1*, 1067-1070.

3. Li, X. L.; Hua, S. Z.; Chopra, H. D.; Tao, N. J. Formation of atomic point contacts and molecular junctions with a combined mechanical break junction and electrodeposition method. *Micro & Nano Letters* **2006,** *1*, 83-88.

4. Kiguchi, M.; Sekiguchi, N.; Murakoshi, K. Electric conductance of metal nanowires at mechanically controllable break junctions under electrochemical potential control. *Surf. Sci.* **2007,** *601*, 5262-5265.

5. Yi, Z. W.; Banzet, M.; Offenhausser, A.; Mayer, D. Fabrication of nanogaps with modified morphology by potential-controlled gold deposition. *Physica Status Solidi-Rapid Research Letters* **2010,** *4*, 73-75.